J Solid State Electrochem (2008) 12:1663–1671
DOI 10.1007/s10008-008-0547-x

ORIGINAL PAPER

Effects of tetrabutylammonium hydrogen sulfate as an electrolyte additive on the electrochemical behavior of lead acid battery

Behzad Rezaei · Mahmood Taki

Received: 29 December 2007 / Revised: 1 March 2008 / Accepted: 2 March 2008 / Published online: 15 April 2008

Abstract Tetrabutyl ammonium hydrogen sulfate is an ion-paring reagent that has similar properties with ionic liquid. Ionic liquids belong to new branch of salts with unique properties that have ever increasing applications in electrochemical systems especially lithium-ion batteries. For the first time, the effects of tetrabutylammonium hydrogen sulfate (TBAHS) as an electrolyte additive in battery's electrolyte was studied on the hydrogen and oxygen evolution overpotential and anodic layer formation on lead–antimony–tin grid alloy of lead acid battery by using cyclic voltammetry and linear sweep voltammetry in aqueous sulfuric acid solution. The grid surface morphology after cyclic redox reaction was studied by using scanning electron microscopy. The results show that, by increasing TBAHS concentration in the electrolyte, hydrogen and oxygen overpotential were increased, and so the crystalline structure of $PbSO_4$ layer changed. Also, cyclic voltammogram on carbon–PbO paste electrode shows that with presence of TBAHS in the electrolyte, oxidation and reduction peak current intensively increased and peak potential for oxidation and reduction of PbO were dependent on TBAHS concentration.

Keywords Lead acid battery · Lead antimony alloy · Hydrogen and oxygen overpotentials · Tetrabutylammonium hydrogen sulfate

B. Rezaei (✉) · M. Taki
Department of Chemistry, Isfahan University of Technology, Isfahan 84156-83111 I.R., Iran
e-mail: rezaei@cc.iut.ac.ir

Introduction

Lead acid battery has been a successful article of commerce for over a century. Its production and use continue to grow because of new application for battery power in energy storage, emergency power, and electric vehicles (including material-handling equipment), and because of continued growth of automobiles, boats, and planes for which it provides the energy for engine starting, vehicle lighting, and engine ignition (SLI) [1]. One of the main problems in lead acid battery is when it is overcharged—it will liberate hydrogen and oxygen gases as water is decomposed. For a battery to be maintenance-free, it is necessary to retard gas liberation; otherwise, the electrolyte would be depleted prematurely and catastrophic failure would result [2]. Also, hydrogen and oxygen gassing, increase risk of explosion and destruction of battery case. To reduce water consumption in maintenance-free batteries, the hydrogen and oxygen evolution overpotentials must be increased by a different strategy that is cited in literature [3–6]. The expander materials are commonly a mixture of inorganic and organic substances that act as dispersant agents by maintaining a highly porous active mass. They also exert other beneficial effects on the behavior of the negative plate by influencing the hydrogen overpotential and inhibiting the effects of impurities [3]. The use of low-antimony or antimony-free alloys is another effective way to minimize gassing and to achieve maintenance-free lead-acid batteries. Thus, new materials have been employed in grid manufacture, e.g., lead–calcium alloy. As little as 0.1% Ca in the lead alloy is sufficient to reduce gassing to a level that the battery can virtually be sealed and no water addition is required [4, 5]. Also, alloying with low amount of tin increased the overvoltage of the oxygen and hydrogen evolution reaction [4]. One of the major problems in the use of lead–calcium–tin

alloys is the control of calcium content. Calcium is very susceptible to oxidation, which is especially severe when the alloy is agitated by stirring, pumping, or is accepting the return of trim strap from cast grids and rejects grids when the temperature at the melt pot is over 450 °C. A solution to the problems associated with calcium fade is given by the addition of minor amounts of aluminum (0.005% to 0.05%) to the lead calcium alloy [5, 7]. In this manner, effect of solidification temperature of lead alloy grids on the electrochemical behavior especially on the overpotential for the evolution of hydrogen gas and on the electrode passivation in sulfuric acid solution was studied [6].

The use of additives in the electrolyte is one of the approaches that offer improvement of the battery without much alteration of other factors. The major problem lies with selecting a suitable additive that is chemically, thermally, and electrochemically stable in highly corrosive environment. Effect of some additives into the paste, grid, and electrolyte of lead acid batteries were investigated on the electrical performance of this kind of batteries [8–15]. Among the additives used so far, the most widely investigated is H_3PO_4 [8, 9], which has been reported as a beneficial additive in terms of improving cyclic life, decreasing self discharge, and increasing the oxygen overpotential on the positive electrode. Other additives, like H_3BO_3 [10] and $SnSO_4$ [11], are also prominent.

Some researchers have investigated the role of sodium sulfate. This additive is added in powder form to the electrolyte in amounts of about 1% of its weight. Sodium sulfate acts by the common ion effect to prevent the harmful depletion of sulfate ion, which is a danger in the discharge of acid-starved batteries. The addition of sodium sulfate provides an 'inventory' of sulfate ions that are available without increasing grid corrosion [12, 13]. Furthermore, some of additives such as amino acids [14], benzaldehyde, and their derivatives [15] were used as a corrosion inhabitation agent for grids.

An ionic liquid (IL) or, classically, a room-temperature molten salt is an interesting series of materials being investigated in a drive to find a novel electrolyte system for electrochemical devices. ILs contain anions and cations, and they show a liquid nature at room temperature without the use of any solvents. The combination of anionic and cationic species in ILs gives them a lot of variation in properties, treated as liquid at ambient temperature, such as thermal stability, nonflammability, high-ion density, wide electrochemical windows, and designable [16]. Because of these unique properties, ILs applicable in many electrochemical devices such as Li ion batteries [17–19], super capacitors [20], solar cells [21], and fuel cells [22].

There are no reports about the application of tetrabutylammonium hydrogen sulfate (TBAHS) on the electrical performance of lead-acid batteries. In this work, effects of TBAHS (Scheme 1) as an additive that is added to electrolyte, the electrochemical properties of lead-acid battery, and especially, the polarization potentials of hydrogen and oxygen evolution gas by using cyclic voltammetric method are investigated.

This IL has many applications in separation technique. For example, it is used as high-performance liquid chromatography mobile phase [23] or ion-pairing reagent in reversed-phase ion-pair chromatography [24, 25]. Furthermore, TBAHS were used as phase transfer catalyst in synthesis of organic compounds when reaction reagents have different hydrophilicity [26, 27].

Experimental

Sulfuric acid, graphite powder, lead oxide, and TBAHS were reagent grade (from Merck), and deionized doubly distilled water was used in preparation of all the solutions. The iron mould with a cooling system and temperature control unit the same as the grid casting machine of Sovema Co. was used for preparing the working electrode. The working electrodes were seven lead–antimony wires with different antimony percentages. The composition of the alloys was Pb–Sb–Sn (X%, Sb; 0.24%, Sn), where X= 0.32, 0.50, 0.73, 1.66, 1.88, 2.50, and 2.80 wt%. The sides and other parts of the working electrodes were covered with an epoxy resin to avoid any contact with the electrolyte solution, except the electrode surface, exposing a 0.50-cm^2 surface area of the alloy.

The electrolyte was 4.0 mol l^{-1} sulfuric acid (normal concentration of sulfuric acid in lead-acid battery), which is prepared from concentrate H_2SO_4 and double-distilled water. Electrolyte solutions contain 2.5, 5.0, 10.0, 15.0, and 20.0 mg ml^{-1}. TBAHS were prepared by adding a known amount of TBAHS salts to the electrolyte. The voltammograms of cyclic voltammetry (CV) and linear sweep voltammetry (LSV) were obtained at a sweep rate

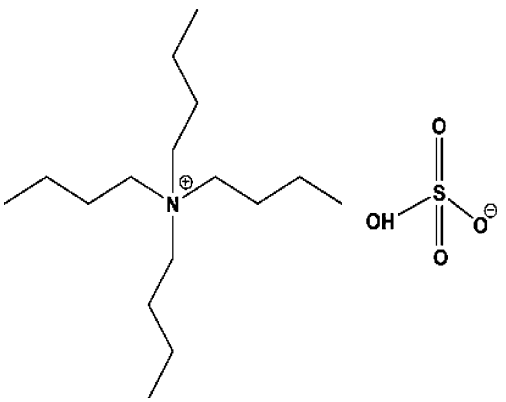

Scheme 1 Molecular structure of tetrabutylammonium hydrogen sulfate (TBAHS)

50.0 mV S^{-1}, in the potential range between hydrogen and oxygen evolution (−2.500 V to +2.500 V vs. saturated calomel electrode, SCE) by using a potentio-galvanostat of Behpajooh Co. Model BHP-2061-C connected to a PC computer. The counter and reference electrodes were platinum black and SCE, respectively. Before the experiment, the electrode was mechanically polished with water-resistant emery paper and washed with acetone and double-distilled water.

After one cycle of CV, the scanning electron micrograph (SEM) technique (Philips-XL30) was applied to study the microstructures of the surface layer on the lead alloy electrodes. Because the morphology of the surface layer must be unchanged and epoxy resin is electrically insulator, a thin layer of Au was deposited on the electrodes before SEM imaging.

Carbon–lead oxide paste electrodes were prepared as follows: 0.20 g of graphite powder, which was washed with ethanol and dried under vacuum, was added to 0.20 g PbO powder and mixed with 0.1 ml of Nujol. This paste was interring into a glass tube with 0.50 cm^2 diameter and pressed to obtain compact structure that its electrical resistance is below 10.0 Ω. Finally, the electrode tip polished with smooth paper and used as working electrode in CV measurements were obtained at a sweep rate 50.0 mV S^{-1}, in the potential range of −0.600 to 1.000 V vs. SCE. The counter and reference electrodes were platinum black and SCE, respectively.

For evaluation of the effects of TBAHS on the corrosion rate of the alloy, LSV and tafel polarization measurement were carried out in the 4.0-mol l^{-1} H_2SO_4 solutions with and without TBAHS. The equilibrium potential (E_{eq}) was determined by immersing Pb–Sb–Sn electrodes and SCE as a working and reference electrode in the 4.0-mol l^{-1} H_2SO_4 solution, and then measuring a different potential after the potential of the specimen becomes stable for a few minutes by using a multimeter. For obtaining tafel plots, the potential was scanned at a rate of 50.0 mV S^{-1} in the cathodic direction between E_{eq} to E_{eq}−350.0 mV, and then in the anodic direction between E_{eq} to E_{eq}+350.0 mV. All experiments were carried out at room temperature (298 K).

Results and discussion

The redox reactions that are occurring on the Pb–Sb–Sn alloy electrodes in sulfuric acid solution are complex and depend on many variables such as the concentration of acid, the sweep rate in CV, and kinds of additives. In this study, particular attention will be paid to the effect of TBAHS as the IL on the hydrogen and oxygen evolution potentials that play an important role in the water consumption of lead acid batteries. On the other hand, the other effects of this additive will be considered.

Figure 1 shows a cyclic voltammogram recorded at a scan rate of 50.0 mV S^{-1} on a Pb-1.6%, Sb-0.24% Sn electrode in the 4.0-mol l^{-1} H_2SO_4 solution with and without TBAHS, in the potential region between hydrogen and oxygen evolution.

According to the literature [28, 29], peaks H and O are assigned to the reduction of hydrogen and oxidation of water that led to hydrogen and oxygen evolution, respectively. Oxidation of Pb to $PbSO_4$ is carried out in A_1, and peak C_1 shows reduction of $PbSO_4$ to Pb. Antimony oxidation in Pb–Sb–Sn alloy begins at the potential value at which PbO formation takes place under $PbSO_4$ membrane [16]. Peaks A_2 and C_3 is related to antimony dissolution and reduction. The reduction of PbO to Pb occurred in C_2 and reduction of PbO_2 to $PbSO_4$ in peak C_4.

The initial reaction of sulfuric acid with lead oxide leads to normal lead sulfate and heat evolution. Under the influence of excess lead oxide and water, this is not stable, so it converts into basic lead sulfate, either tribasic lead sulfate ($3PbOPbSO_4$) or tetrabasic lead sulfate. ($4PbOPbSO_4$). Tribasic lead sulfate is crystallized as small needles with high specific surface; however, tetrabasic lead sulfate forms more bulky crystals [30]. TBAHS dissolves in electrolyte and tetrabulyl ammonium (TBA^+), and hydrogen sulfate would result. Hydrogen sulfate is a common ion. Therefore, the effects of TBAHS is because of TBA^+ ion in electrolyte. Interaction between this cation and the electrode surface change the structures of basic lead sulfate formed on surface electrode and other electrochemical changes would result.

Corresponding to the results which are obtained from Fig. 1, the addition of TBAHS to the electrolyte increased hydrogen and oxygen overpotentials in about 0.20 V for hydrogen and 0.08 V for oxygen overpotential. To consider

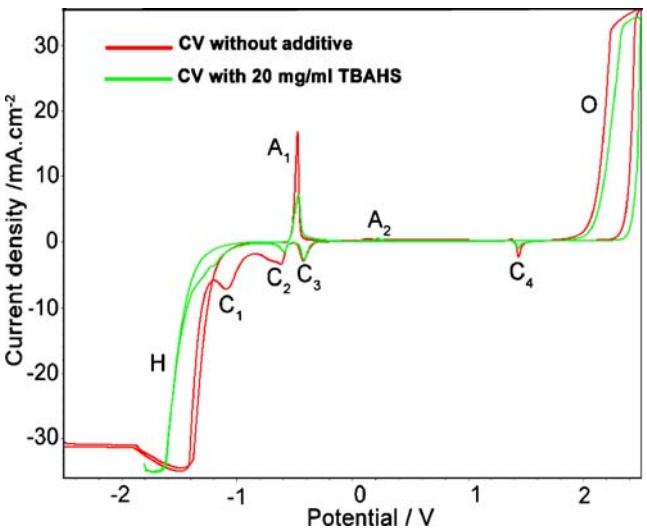

Fig. 1 Cyclic voltammogram of Pb-1.6%, Sb-0.24% Sn alloy at the scan rate of 50 mV S^{-1} in 4.0 mol l^{-1} H_2SO_4 with and without TBAHS

the catalytic effect of antimony on hydrogen and oxygen evolution potential, this potential in the first scan of linear sweep voltammogram depicts antimony percent in the alloys at several current density and five different concentrations of TBAHS. The results show a similar trend in hydrogen evolution potential in all current densities. As SLI batteries are employed at high current density, Fig. 2 was obtained at the current density of 30.0 mA cm^{-2}. This figure shows that antimony in the alloy, lower hydrogen overpotential, and its effect does not change with TBAHS. Oxygen overvoltage is scarcely dependent on the Sb contents. It depends on the film characteristics because it takes place on the PbO_2 film.

Water loss in the batteries that use Pb–Sb–Sn alloy to produce the positive and negative grid has been high because antimony from the positive grid can migrate through the electrolyte and be deposited on the surface of the negative plate, where it diminishes the overpotential for hydrogen evolution [30]. For this reason, in a maintenance-free battery, the grid is made of low-antimony alloy (1–2 wt.%). Therefore, in this study, the other experiments were carried out on the Pb-1.6%, Sb alloy. The effect of concentration of TBAHS in the range of 2.5–20.0 mg ml^{-1} on hydrogen and oxygen overpotentials is shown in Fig. 3. It has been seen that, with increasing TBAHS concentration of up to 2.5 mg ml^{-1}, hydrogen overvoltage is increased and then remain constant. The linear sweep voltammograms of hydrogen overpotential in different concentrations of TBAHS are shown in Fig. 4. The potential for oxygen evolution depends on the film characteristics because it takes place on the PbO_2 film; thus, we observe for Pb–Sb–Sn electrodes irregular behavior in all TBAHS concentrations. Therefore, with the

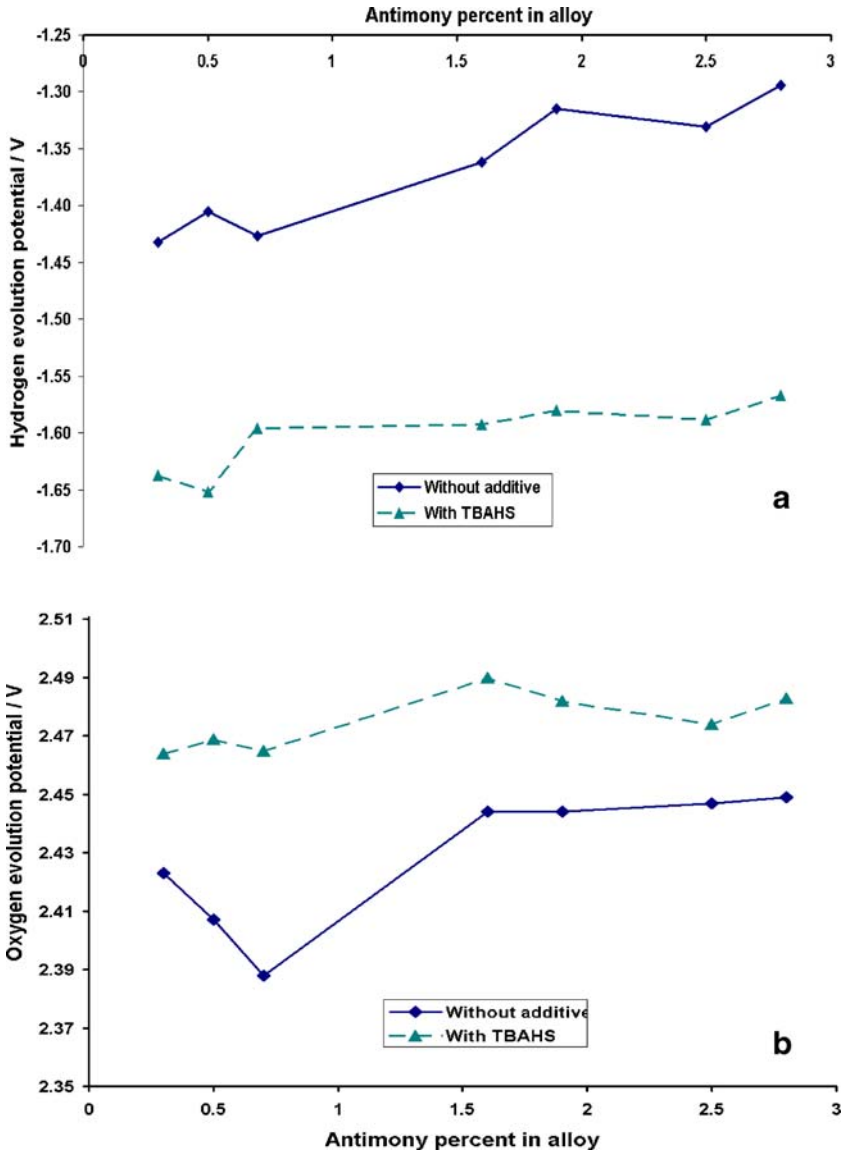

Fig. 2 Increase hydrogen (**a**) and oxygen (**b**) overpotential with TBAHS additive in electrodes with several antimony percents in current density of 30.0 mA cm^{-2} and 4.0 mol l^{-1} H_2SO_4

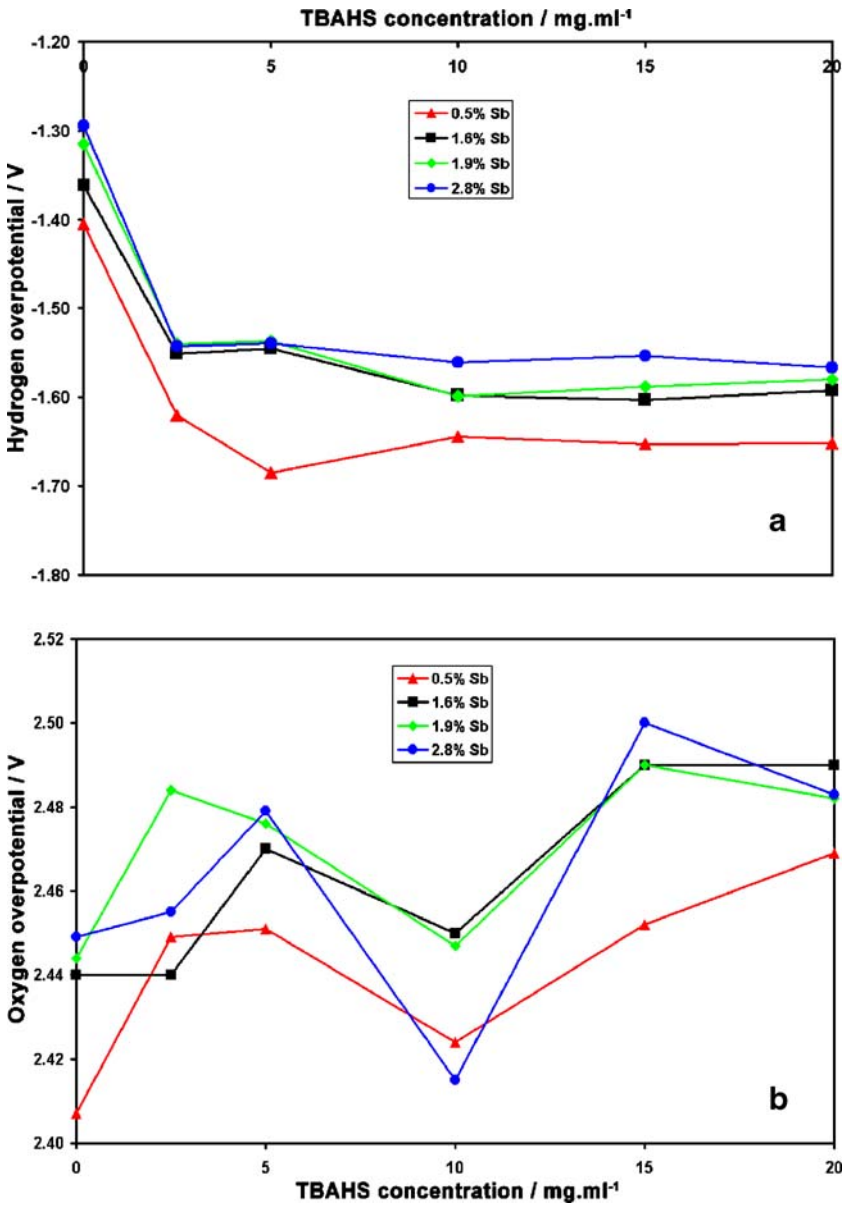

Fig. 3 **a** Hydrogen and **b** oxygen overpotential in 4.0 mol l^{-1} H_2SO_4 with various TBAHS concentrations

presence of TBAHS as an electrolyte additive, hydrogen and oxygen overpotential has been increased so water decomposition and consumption decreased.

According to Fig. 1, TBAHS in acid solution decreases the peak current of Pb to $PbSO_4$, which indicates smaller $PbSO_4$ formed on electrode surface in comparison with the solution without additive. In Fig. 5a and b, the SEMs of the lead–antimony electrodes after using one cycle of charge and discharge in sulfuric acid solution with and without TBAHS are demonstrated. The results show that (a) the crystals that formed on lead alloy in solution with TBAHS are smaller in size than those on electrolyte without additive. The average diameter of crystals formed on the solution without TBAHS is 0.82 μm; however, in electrolyte with additive, the average diameter size is 0.42 μm. (b) The distribution of $PbSO_4$ crystals that are formed in the solution with TBAHS is uniform and covers a larger surface area of the electrode. However, SEM images show that $PbSO_4$ crystals cover almost the entire electrode surface and have smaller crystal size, and approve the result obtained from Fig. 1. Regarding the SEM image, it is concluded that diminished conversion of Pb to $PbSO_4$ in TBAHS solution decreases surface sulfatation. However, evenly distributed $PbSO_4$ crystal on the electrode surface results to electrode passivation and smaller surface area exposed to the electrolyte that might increase hydrogen and oxygen overpotentials.

It has been pointed out by Pavlov [31, 32] and Ruetschi [33] that the $PbSO_4$ film on Pb acts as a perm-selective membrane that becomes impermeable to SO_4^{2-} and HSO_4^- when it has reached a thickness of 1 to several micrometers.

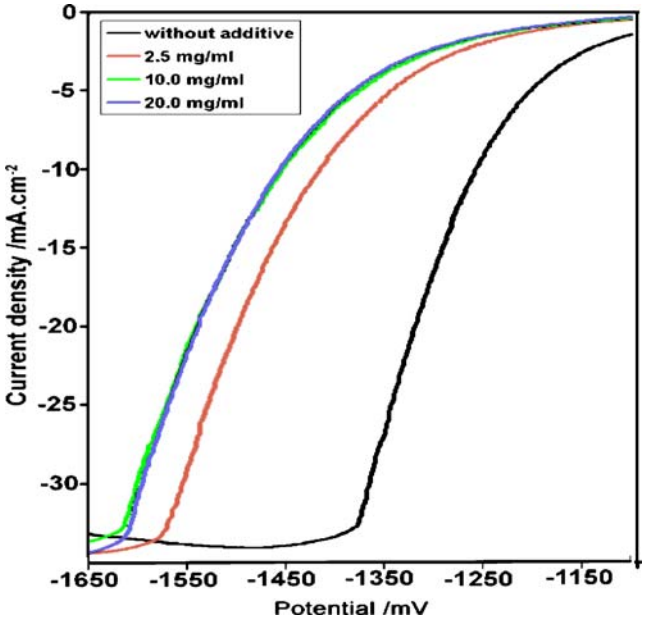

Fig. 4 The linear sweep voltammograms (LSV) of Pb-1.6%, Sb-0.24% Sn alloy in negative potential direction scanning for various TBAHS concentrations. Scan rate, 50.0 mV S^{-1}, H_2SO_4 4.0 mol l^{-1}

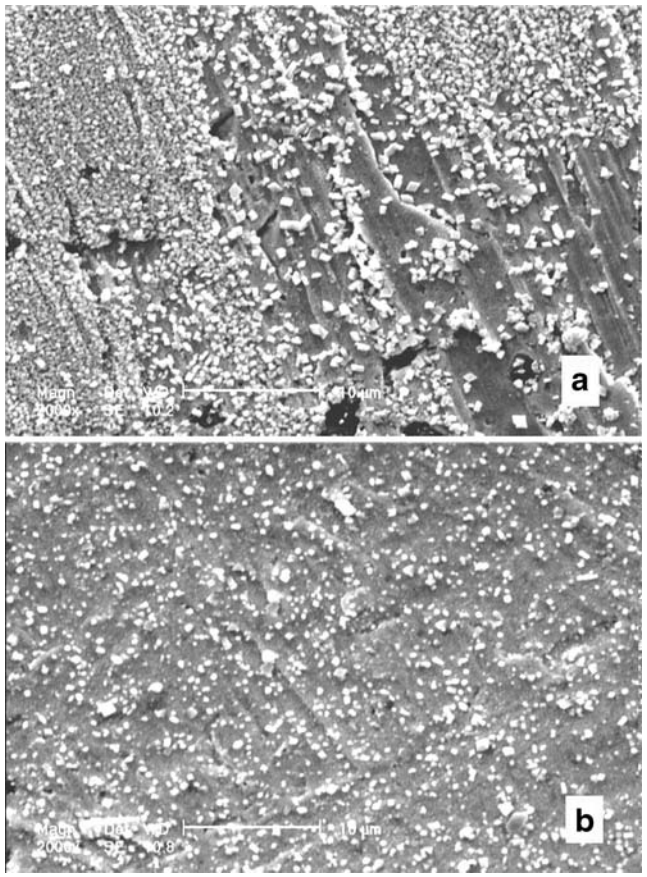

Fig. 5 The scanning electron micrographs (SEM) after using one cycle of charge and discharge for Pb-1.6%, Sb-0.24% Sn alloy in 4.0 mol l^{-1} H_2SO_4 (**a**), without additive (**b**), with 5.0 mg ml^{-1} TBAHS

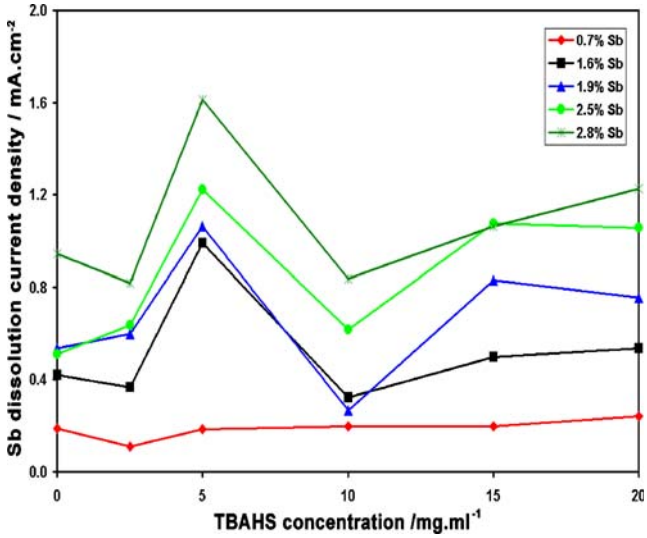

Fig. 6 Effect of TBAHS concentration on antimony dissolution current density

Only the migration and diffusion of the H^+ or OH^- ions through the $PbSO_4$ intercrystalline spaces can occur to carry the current. Therefore, underneath the $PbSO_4$ membrane, the pH increases, and tetragonal lead monoxide (tetra-PbO) and basic lead sulfates are formed. Higher porosity of the $PbSO_4$ formed on Pb–Sb–Sn alloys rather than on pure Pb was noticed by many authors [33–37] and was confirmed by the examination of a microstructure of the Pb–Sb–Sn alloys and morphology of the $PbSO_4$ crystals [38–40], as well as by the impedance measurements [41]. A higher $PbSO_4$ porosity means that the $PbSO_4$ layer becomes less perm-selective, preventing the pH to rise to the same extent as on a pure-Pb electrode.

The SEM image in Fig. 5b shows similarly formed crystals as the tribasic lead sulfate structure, which has high specific surface and covers more surface area of the

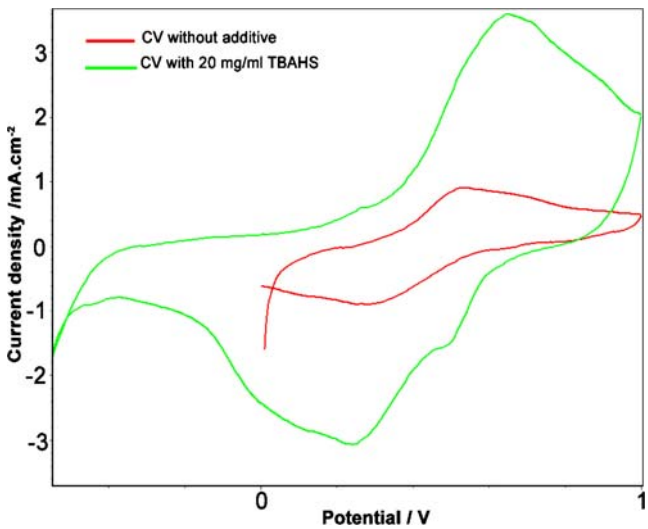

Fig. 7 Cyclic voltammogram of carbon/PbO paste electrode in 4.0 mol l^{-1} H_2SO_4 with and without TBAHS (ν=50.0 mV S^{-1})

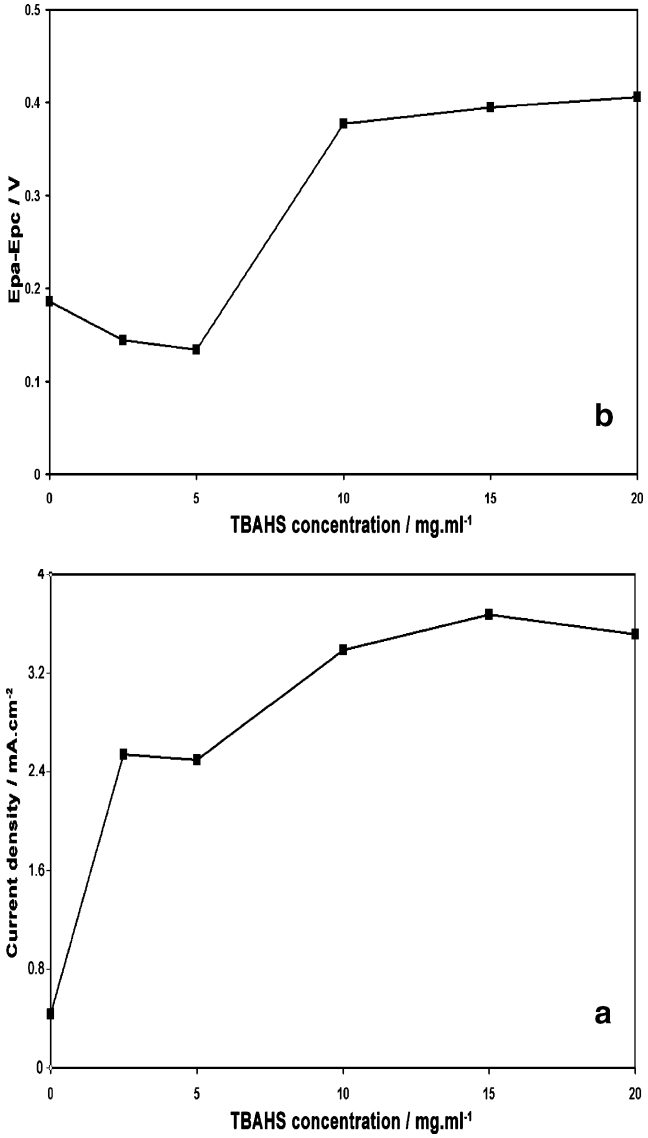

Fig. 8 Peak current (**a**) and peak potential difference (reversibility) (**b**) according to TBAHS concentration

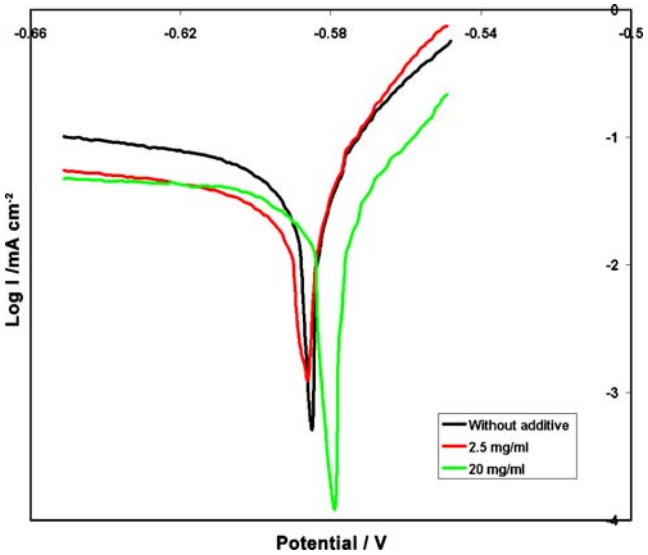

Fig. 9 Effect of TBAHS on lead alloy polarization curves in 4.0 mol l^{-1}

electrode. Therefore, the existence of TBAHS in the electrolyte increases electrode passivation. This result might be proven by voltammetric measurements. TBAHS decreases the porosity of $PbSO_4$ perm-selective membrane, and diffusion of ions through the passivation layer becomes slow and makes the actual electrode area decrease so that less basic lead sulfate and tetra-PbO are formed on the electrode surface. This is approved by the diminution current peaks of Pb to $PbSO_4$ and tetra-PbO to Pb in peaks A_1 and C_2 in Fig. 1.

In recrystallization and self-discharge, many big $PbSO_4$ crystals are formed on a seriously passivated negative plate. The micro-pores in the active mass became very narrow and long, and even their passageways are greatly blocked. The porosity in the active mass decreases obviously. The mass transfer of ions in it becomes very difficult. In charge/discharge cycles, many small $PbSO_4$ crystals are formed over the big crystals that are very difficult to reduce [42]. Two reduction peaks of $PbSO_4$ appear clearly on the negative-going potential sweep curves. They represent the reduction of $PbSO_4$ crystals of different sizes. The more-negative reduction peak is the reduction of the big $PbSO_4$ crystals. The electrode surface is covered by many small $PbSO_4$ crystals. The reduction rate of the negative active mass is controlled by the diffusion process of the SO_4^{2-} ion from the depth of the micro-pores to the bulk solution. When the active mass on the negative plate is passivated seriously, the passageway in the micro-pores becomes so small that the shifting of the peak potential of the $PbSO_4$ reduction in the negative direction exceeds 200 mV [43]. It seems that the tetrabutyl ammonium cation, because of its large size, blocks the passageway in the micro-pores and decreases the diffusion rate of the SO_4^{2-} ion, and led to formation of more smaller crystals. For this reason, with TBAHS in electrolyte, peak current of C_1 in Fig. 1 becomes smaller, which verifies the smaller $PbSO_4$ crystals that was formed in TBAHS the solution.

Table 1 Corrosion data for Pb-1.6%, Sb alloy in 4.0 mol l^{-1} H_2SO_4 in the presence and absence of TBAHS obtained by the Tafel polarization method

TBAHS concentration (mg ml^{-1})	E_{corr} (V)	i_{corr} (μA cm^{-2})	Inhibition efficiency (%)	Corrosion rate (mpy)
0 (without additive)	−0.580	57.1	–	67
2.5	−0.588	44.7	22.4	52
10.0	−0.579	48.9	14.9	57
20.0	−0.572	50.1	13.4	58

Just as stated previously, Sb dissolution in the alloy lowers the overpotential for hydrogen evolution [30]. The change of antimony dissolution current versus TBAHS concentration has been shown in Fig. 6. No regular changes have been seen in Sb dissolution, with the presence of this additive in electrolyte.

The electrochemical effects of TBAHS in the conversion of PbO to Pb and PbO_2 were investigated by carbon/PbO electrode. Cyclic voltammogram of the paste electrode is shown in Fig. 7. Figure 8 shows the current peak of PbO to Pb^{2+} and E_{pa}–E_{pc} according to TBAHS concentration. The results indicate that addition of this IL to the battery electrolyte increases current conversion of PbO to Pb^{2+} and PbO_2. Interaction between Pb^{2+} and TBAHS ions make more stable species of Pb^{2+}. Therefore, dissolution of PbO to Pb^{2+} increased, which led to increased current conversion of PbO to Pb^{2+}. In a lower concentration of TBAHS, the reversibility of redox reaction increased, which is a beneficial effect in the negative and positive active material of the battery.

The effects of this additive on grid corrosion rate have been considered. Figure 9 shows the polarization curves of lead–antimony alloy with and without the presence of TBAHS, and corresponding corrosion data are given in Table 1. These results show that TBAHS in electrolyte acts as a corrosion inhibitor. With addition of TBAHS, corrosion rate decreased, but when its concentration increased, the corrosion inhibitor effect will be a little insignificant. Also, with this additive, the corrosion potential has been decreased because of the interaction between TBA^+ ion and the electrode surface. The following equation was used to calculate the inhibitor efficiency (IE) from polarization measurements:

$$IE = \left(1 - \frac{i}{i_o}\right) \times 100$$

where i_0 and i are the corrosion current densities (mA cm^{-2}) obtained by extrapolation of the cathodic and anodic Tafel line in solution with and without TBAHS. As stated previously, this IL causes tribasic lead sulfate formation, which covers more electrode surface area and less electrode surface exposed to electrolyte, resulting decreased grid corrosion rate.

Conclusion

An effect of TBAHS as an electrolyte additive was investigated on the electrochemical properties of lead-acid battery. The investigation was performed by CV and SEM. CV was performed to investigate the effect of TBAHS on the surface characteristics of lead–antimony electrode and the polarization potential of oxygen gas evolution. The electrochemical behavior of electrodes depends on TBAHS concentration in the electrolyte solution. Therefore, these electrodes show different electrochemical behavior (mainly different polarization potential for hydrogen and oxygen evolution). Also, in higher TBAHS concentration, we observe greater polarization potential for hydrogen and oxygen evolution, and the remaining crystals after cycle of charge and discharge is higher.

Acknowledgment The authors acknowledge the Isfahan University of Technology Council and the Center of Excellency in Sensor and Green Chemistry for supporting this work.

References

1. Linden D, Reddy TB (2002) Handbook of batteries, 3rd edn, vol. 23, p 1
2. Crompton TR (2000) Battery reference book, 3rd edn, vol. 18, p. 5
3. Francia C, Maja M, Spinelli P (2001) J Power Sources 95:119
4. Bui N, Mattesco P, Simon P, Steinmetz J, Rocca E (1997) J Power Sources 67:61
5. Hibbins SG, Timpano FA, Zuliani DJ (1996) US Patent 5,547,634
6. Rezaei B, Damiri S (2005) J Solid State Electrochem 9:590
7. Zhong S, Liu HK, Dou SX, Skyllas-Kazacos M (1996) J Power sources 59:123
8. Pavlov D (1993) J Power Sources 42:345
9. Garche J, Doring H, Wiesener K (1991) J Power Sources 33:213
10. Badawy WA, El-Egamy SS (1995) J Power Sources 55:11
11. Voss E, Hullmeine U, Winsel A (1990) J Power Sources 30:33
12. Ferreira AL (2001) J Power Sources 94:255
13. Weighall MJ (2003) J Power Sources 116:219
14. Ghasemi Z, Tizpar A (2006) Appl Surf Sci 252:3667
15. Dietz H, Hoogestraat G, Laibach S, von Borstel D, Wiesener K (1995) J Power Sources 53:359
16. Ohno H (2005) Electrochemical aspects of ionic liquids. Wiley, New York
17. Sakaebe H, Matsumoto H, Tatsumi K (2007) Electrochim Acta 53:1048
18. Ishikawa M, Sugimoto T, Kikuta M, Ishiko E, Kono M (2006) J Power Sources 162:658
19. Markevich E, Baranchugov V, Aurbach D (2006) Electrochem Commun 8:1331
20. Balducci A, Bardi U, Caporali S, Mastragostino M, Soavi F (2004) Electrochem Commun 6:566
21. Dai Q, Menzies DB, MacFarlane DR, Batten SR, Forsyth S, Spiccia L, Cheng YB, Forsyth M (2006) C R Chimie 9:617
22. De Souza RF, Padilha JC, Gonc_alves RS, Dupont J (2003) Electrochem Commun 5:728
23. Upreti VV, Khurana M, Cox DS, Eddington ND (2006) J Chromatography B 831:156
24. Vanerkova D, Jandera P, Hrabica J (2007) J Chromatography A 1143:112
25. Yang X, Hu Z, Yung Chan S, Cher Goh B, Duan W, Chan E, Zhou S (2005) J Chromatography B 821:221
26. Liu B, Hu XL, Liu J, Zhao YD, Huang ZL (2007) Tetrahedron Lett 48:5958
27. Tewari N, Dwivedi N, Tripathi RP (2004) Tetrahedron Lett 45:9011

28. Hirasawa T, Sasaki K, Taguchi M, Kanecho H (2000) J Power Sources 85:44
29. Babic R, Melikos-Hukoric M, Lajqy N, Brinic S (1994) J Power Sources 52:17
30. Rusin AI (1987) Modern technology of lead-acid batteries. Energiya, Leningrad, p 182
31. Culpin B, Rand DAJ (1991) J Power Sources 36:415
32. Pavlov D (1968) Electrochim Acta 13:2051
33. Pavlov D, Popova R (1970) Electrochim Acta 15:1483
34. Ruetschi P (1973) J Electrochem Soc 120:331
35. Sharpe TF (1977) J Electrochem Soc 124:168
36. Hampson NA, Kelly S, Peters K (1980) J Appl Electrochem 10:91
37. Ijomah MN (1987) J Electrochem Soc 134:1960
38. Webster S, Mitchell PJ, Hampson NA, Dyson DI (1986) J Electrochem Soc 133:137
39. Pavlov D, Monahov B (1991) J Electroanal Chem 305:57
40. Pavlov D, Monahov B (1987) J Electroanal Chem 218:135
41. Gaad Allah AG, El-Rahman HAA, Salih SA, El-Galil MA (1992) J Appl Electrochem 22:571
42. Guo Y, Chen J, Li L (1992) J Electrochem Soc 139:L–99
43. Brennan MPJ, Stirrup BN, Hampson NA (1974) J Appl Electrochem 4:497